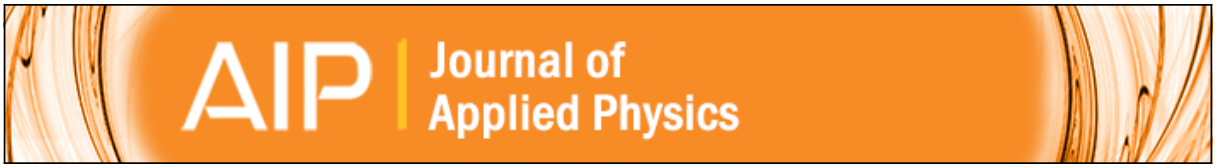

Influence of H on the composition and atomic concentrations of "N-rich" plasma deposited SiO x N y H z films

A. del Prado, E. San Andrés, I. Mártil, G. González-Daz, W. Bohne, J. Röhrich, and B. Selle

Citation: Journal of Applied Physics **95**, 5373 (2004); doi: 10.1063/1.1699525
View online: http://dx.doi.org/10.1063/1.1699525
View Table of Contents: http://scitation.aip.org/content/aip/journal/jap/95/10?ver=pdfcov
Published by the AIP Publishing

Influence of H on the composition and atomic concentrations of "N-rich" plasma deposited $SiO_xN_yH_z$ films

A. del Prado,[a] E. San Andrés, I. Mártil, and G. González-Díaz
Departamento Física Aplicada III, Universidad Complutense de Madrid, 28040, Madrid, Spain

W. Bohne, J. Röhrich, and B. Selle
Abt. Silizium-Photovoltaik und Ionenstrahl-Labor, Hahn-Meitner-Institut, 12489, Berlin, Germany

(Received 26 January 2004; accepted 18 February 2004)

The influence of H on the composition and atomic concentrations of Si, O, and N of plasma deposited $SiO_xN_yH_z$ films was investigated. The bonding scheme of H was analyzed by Fourier-transform infrared spectroscopy. The composition and absolute concentrations of all the species present in the $SiO_xN_yH_z$, including H, was measured by heavy-ion elastic recoil detection analysis (HI–ERDA). Samples were deposited from SiH_4, O_2, and N_2 gas mixtures, with different gas flow ratios in order to obtain compositions ranging from SiN_yH_z to SiO_2. Those samples deposited at higher SiH_4 partial pressures show both Si–H and N–H bonds, while those deposited at lower SiH_4 partial pressures show N–H bonds only. The Si–H and N–H bond concentrations were found to be proportional to the N concentration. The concentration of H was evaluated from the Si–H and N–H stretching absorption bands and compared to the HI–ERDA results, finding good agreement between both measurements. The deviation from H-free stoichiometric SiO_xN_y composition due to the presence of N–H bonds results in an effective coordination number of N to produce Si–N bonds lower than 3. By fitting the experimental composition data to a theoretical model taking into account the influence of N–H bonds, the actual concentration of N–H bonds was obtained, making evident the presence of nonbonded H. The presence of Si–H and Si–Si bonds was found to partially compensate the effect of N–H bonds, from the point of view of the relative N and Si contents. Finally, the presence of N–H bonds results in a lower Si atom concentration with respect to the stoichiometric film, due to a replacement of Si atoms by H atoms. This decrease of the Si concentration is lower in those films containing Si–H and Si–Si bonds. A model was developed to calculate the Si, O, and N atom concentrations taking into account the influence of N–H, Si–H, and Si–Si bonds, and was found to be in perfect agreement with the experimental data measured by HI–ERDA. © *2004 American Institute of Physics.* [DOI: 10.1063/1.1699525]

I. INTRODUCTION

Interest in silicon oxynitride ($SiO_xN_yH_z$) is continuously increasing due to its many electrical and optical applications. When used as gate dielectric in metal–insulator–semiconductor devices, the higher dielectric permitivity of $SiO_xN_yH_z$ with respect to SiO_2 allows higher physical thickness with the same capacitance–voltage characteristic, thus reducing tunneling leakage currents.[1] Additionally, the presence of N results in better barrier properties against the diffusion of boron and alkali ions[1] and improves the reliability of the devices.[2] By an adequate control of the composition of $SiO_xN_yH_z$, it is possible to greatly reduce the mechanical stress with respect to SiN_yH_z, making the $SiO_xN_yH_z$ a suitable insulator in multilevel metallization processes[3] and lithography applications.[4] Finally, the control of the refractive index of $SiO_xN_yH_z$ between the values of SiN_yH_z and SiO_2 allows many interesting optical applications, such as graded index films or antireflection coatings.[5–7]

Owing to the possibility to deposit films at low temperature, one of the most frequently used methods for the growth of $SiO_xN_yH_z$ films is the plasma enhanced chemical vapor deposition (PECVD),[3,8,9] with the remote PECVD[1,10,11] and the electron cyclotron resonance (ECR–PECVD)[5,12–14] variants. In these techniques precursor gases containing H, such as SiH_4 and NH_3, are frequently used, so that H is incorporated into the films. This H results in deviations of the composition and the density of the films with respect to stoichiometric SiO_xN_y and has an influence on the film properties, such as the refractive index,[15] as well as playing an important role on the thermal stability of the films.[16,17]

In this article the incorporation of H into $SiO_xN_yH_z$ films deposited by ECR–PECVD from SiH_4, O_2, and N_2 gas mixtures is studied and discussed in detail. The absolute concentrations of all the species present in the $SiO_xN_yH_z$, including H, were accurately measured by heavy-ion elastic recoil detection analysis (HI–ERDA) and compared to the expected values for H-free stoichiometric SiO_xN_y. The observed differences are satisfactorily explained by taking into account the concentration and the bonding scheme of the H present in our $SiO_xN_yH_z$ films, allowing the development of a model to explain the influence of H on the composition of the $SiO_xN_yH_z$ films and on the absolute atomic concentrations of Si, O, and N.

[a]Electronic mail: alvarop@fis.ucm.es

II. EXPERIMENT

The $SiO_xN_yH_z$ films were deposited from SiH_4, O_2, and N_2 gas mixtures, using a commercial ECR reactor (Astex AX4500) attached to a stainless steel deposition chamber. The deposition system is described in detail elsewhere.[18,19]

In all depositions the total gas flow, pressure, and microwave power were kept constant at 10.5 sccm, 9×10^{-4} mbar, and 100 W, respectively. The deposition temperature was about 50 °C, as the substrates were not intentionally heated. The samples were deposited on high resistivity (80 Ω cm) *p*-type Si (111) substrates. The substrates were cleaned using standard procedures.[20] The thickness of the films was about 300 nm.

Two series of $SiO_xN_yH_z$ samples were deposited using different SiH_4 partial pressures, so that for each series H is incorporated in a different bonding scheme. One series of samples was deposited setting the parameter $R=[\phi(O_2)+\phi(N_2)]/\phi(SiH_4)$ at $R=5.0$, which means a relatively low SiH_4 partial pressure, and changing the parameter $Q=\phi(O_2)/\phi(SiH_4)$ from $Q=0$ (no O_2) to $Q=5.0$ (no N_2) in order to obtain compositions ranging from SiN_yH_z to SiO_2. $\phi(O_2)$, $\phi(N_2)$, and $\phi(SiH_4)$ are the gas flows of O_2, N_2, and SiH_4, respectively. The second series was deposited at $R=1.6$, which means a higher SiH_4 partial pressure (and, therefore, a higher Si content in the films),[21] and changing Q from $Q=0$ to $Q=1.6$.

The composition of the films was measured using the HI–ERDA technique, irradiating the samples with 150 MeV ^{86}Kr ion beams from the ion beam facility of the Hahn-Meitner-Institut, Berlin. The identification of the recoiled species was performed using the time-of-flight mass separation technique. This technique allows the determination of the absolute area concentrations (atoms/cm^2) of all the species present in the $SiO_xN_yH_z$ films, including H, without need of any reference sample, with a very high sensitivity (0.01 at. %) and precision (about 3%). Details on the HI–ERDA setup and the measurements are given elsewhere.[22,23]

The bonding structure of the films was investigated by Fourier-transform infrared (FTIR) spectroscopy. All films were analyzed using a Nicolet Magna-IR 750 series II spectrometer and a Perkin Elmer System 2000 spectrometer, working in the transmission mode at normal incidence. Very good agreement between both measurements was observed.

The thickness of the films was measured by ellipsometry using a Plasmos E2302 ellipsometer with incidence and detection angles both set at 70°. The absolute volume concentrations (atoms/cm^3) of the different species (Si, O, N, and H) were obtained using the area density provided by the HI–ERDA measurements and the thickness.

III. RESULTS AND DISCUSSION

A. Stoichiometric SiO_xN_y

Before presenting the results obtained and discussing the deviations from the stoichiometric composition due to the presence of H, it is convenient to define stoichiometric SiO_xN_y.

By stoichiometric SiO_xN_y we understand a film in which each Si atom has its four bonds saturated with O and/or N atoms. So, in a stoichiometric SiO_xN_y film the only possible bonds are Si–O and Si–N, and there is no H present in the film. According to this definition, and taking into account the coordination numbers of each atom, the following relationships between the Si, O, and N stoichiometric atom concentrations ($[Si]_0$, $[O]_0$, and $[N]_0$, respectively) and the concentrations of Si–O and Si–N bonds ($[Si–O]_0$ and $[Si–N]_0$) must be satisfied:

$$4[Si]_0=[Si–O]_0+[Si–N]_0, \tag{1a}$$

$$2[O]_0=[Si–O]_0, \tag{1b}$$

$$3[N]_0=[Si–N]_0. \tag{1c}$$

Equations (1a)–(1c) lead to the following characteristic linear relationship between the indexes $x=[O]_0/[Si]_0$ and $y=[N]_0/[Si]_0$ for stoichiometric SiO_xN_y films:

$$2x+3y=4. \tag{2}$$

Additionally, for these stoichiometric films, a characteristic composition parameter (α_0) providing information about how close the composition is to either SiO_2 or Si_3N_4 can be defined as the fraction of Si–O bonds with respect to the total number of Si bonds (i.e., $[Si–O]_0+[Si–N]_0$):

$$a_0=\frac{[Si–O]_0}{[Si–O]_0+[Si–N]_0}=\frac{2x}{2x+3y}. \tag{3}$$

The meaning of this parameter may be clarified by rewriting the SiO_xN_y formula in the following way:

$$SiO_xN_y\leftrightarrow(SiO_2)_{\alpha_0}(SiN_{4/3})_{1-\alpha_0}. \tag{4}$$

So, α_0 accounts for the ''oxide fraction'' in the SiO_xN_y film, with $\alpha_0=0$ for Si_3N_4; $\alpha_0=1$ for SiO_2; and $\alpha_0=0.5$ for the middle composition. [It must be noted that writing the SiO_xN_y formula as shown in Eq. (4) does not imply separation of two phases in the film. Likewise, we use the terms ''oxide fraction'' or ''nitride fraction'' when writing the SiO_xN_y formula using the composition parameter α_0, but it does not mean that a separation of a silicon oxide phase and a silicon nitride phase actually exists. In a previous work we showed that the films deposited at the conditions used in this work are essentially single-phase homogeneous films, with a structure of bonds in accordance with the random bonding model.][21]

In practice, it is true that O–O, N–N, and O–N bonds are not present in $SiO_xN_yH_z$ films, due to their low binding energy.[9,24] However, deviations from the stoichiometric composition are indeed possible due to the presence of Si–Si bonds,[24] as well as Si–H, N–H, and even O–H bonds when H is incorporated into the films during the deposition process. These deviations, specially the influence of H, will be discussed along the article.

B. FTIR results

FTIR spectroscopy measurements were performed in order to determine the bonding scheme of H in our $SiO_xN_yH_z$ films. Figure 1 shows the high frequency part of the absorption spectrum for some representative samples. In those films

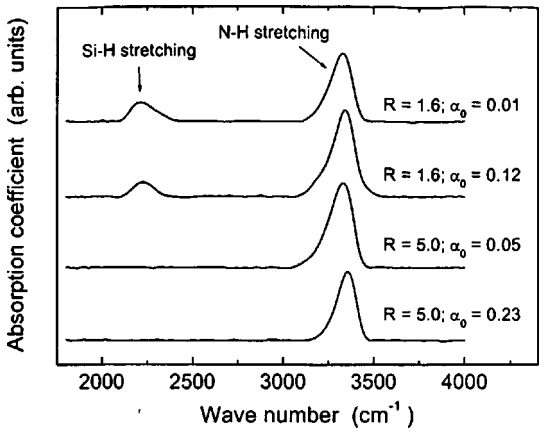

FIG. 1. Absorption spectra in the 2000–4000 cm^{-1} range for some representative samples.

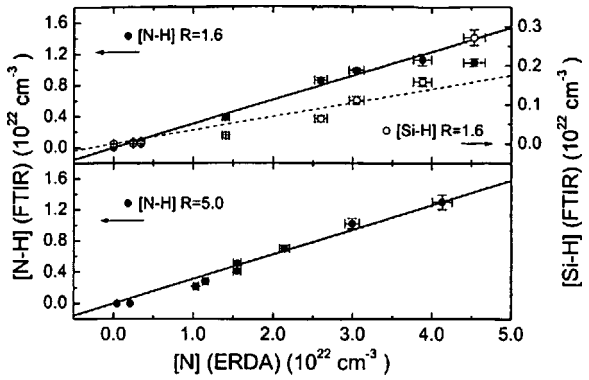

FIG. 3. Concentration of N–H and Si–H bonds, obtained by FTIR, as a function of the N atom concentration, obtained by HI–ERDA, and linear fit of the data.

deposited at $R=1.6$, both Si–H and N–H bonds were detected with a significantly higher N–H concentration, while the films deposited at $R=5.0$ show N–H bonds only. No O–H bonds were detected in any sample. The presence of Si–H bonds only in those samples deposited at $R=1.6$ is due to the higher SiH_4 partial pressure during the deposition, which results in a higher Si content of the films.[21]

The concentration of Si–H and N–H bonds was evaluated from the area of the Si–H and N–H stretching bands, using the calibration factors provided by Lanford and Rand[25]

$$[\mathrm{H}]=[\mathrm{Si{-}H}]+[\mathrm{N{-}H}]=1.36\times10^{17}\times\frac{A_{\mathrm{SiH}}+1.4A_{\mathrm{NH}}}{d}\ \ \mathrm{cm}^{-3}, \tag{5}$$

where A_{SiH} and A_{NH} are the areas of the Si–H and N–H stretching bands, respectively, and d is the thickness of the film.

Figure 2 shows these Si–H and N–H bond concentrations as a function of the composition parameter α_0 [Eq. (3)], obtained from the HI–ERDA measurements. As shown in the figure, both the Si–H and the N–H bond concentrations decrease as the composition changes from $SiN_yH_z(\alpha_0=0)$ to $SiO_2(\alpha_0=1)$. In the case of the N–H bonds, the observed decrease is directly correlated to the decrease of the N content as α_0 changes from 0 to 1. In fact, the N–H concentration is proportional to the N atom concentration measured by HI–ERDA. This relationship is shown in Fig. 3 for the films deposited at $R=1.6$ (up) and $R=5.0$ (down). The solid lines in the figures correspond to the linear fit

$$[\mathrm{N{-}H}]_{\mathrm{FTIR}}=C_{\mathrm{NH}}[\mathrm{N}] \tag{6a}$$

and the obtained results for C_{NH} are:

$$R=1.6: \quad C_{\mathrm{NH}}=0.307\pm0.008, \tag{6b}$$

$$R=5.0: \quad C_{\mathrm{NH}}=0.315\pm0.011. \tag{6c}$$

In the case of the films deposited at $R=1.6$, the sample with the highest N content slightly deviates from the general trend and it has not been taken into account for the fitting calculation.

Concerning the Si–H concentration, a proportional relationship with the Si concentration, analogous to Eq. (6a), was not observed. This result is evidenced in Fig. 2 by the Si–H bond concentration dropping below the detection limit (about 10^{20} cm^{-3}) for high values of $\alpha_0(\alpha_0>0.8)$, despite the Si content remains above the 33 at. % value, corresponding to $SiO_2(\alpha_0=1)$.

This behavior is a consequence of the deposition conditions during the growth of this sample series. The SiH_4 partial pressure is kept constant while the partial pressures of O_2 and N_2 are changed to obtain compositions ranging from SiN_yH_z to SiO_2. Si–H bonds are formed when there is excess SiH_4 which is not consumed by the N_2 or O_2 present in the deposition chamber.[14,21] For the sample deposited at $Q=0$ (no O_2 during the deposition), not all the SiH_4 is consumed by the N_2 to produce Si–N and N–H bonds, and some Si–H (and most likely also Si–Si) bonds are formed. However, when the O_2 partial pressure is increased, the higher reactivity of O_2 with respect to N_2 results in a decrease of the available excess SiH_4, so that the Si–H bond concentration decreases below the detection limit.

So, it is the increase of the O_2 partial pressure with respect to the SiH_4 partial pressure (i.e., the deposition parameter Q) which is responsible for the decrease of the Si–H concentration. As the parameter Q also determines the relative incorporation of O and N (i.e., determines the value of the composition parameter α_0),[21,23] for a sample series deposited at a constant SiH_4 partial pressure, there is a relation-

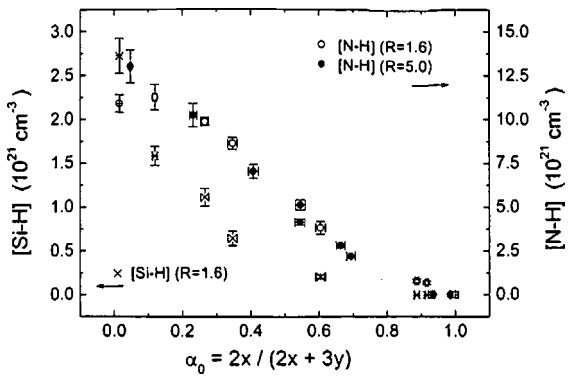

FIG. 2. Concentration of Si–H and N–H bonds as a function of the composition parameter α_0.

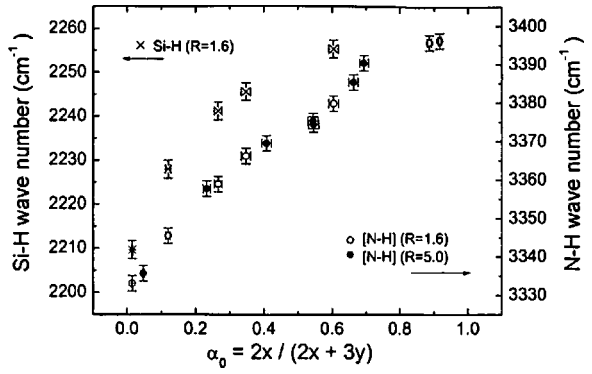

FIG. 4. Wave number of the N–H and Si–H stretching bands as a function of the composition parameter α_0, obtained by HI–ERDA, for the films deposited at $R=1.6$ and $R=5.0$.

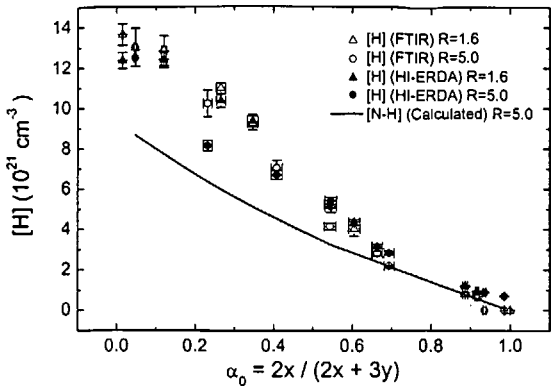

FIG. 5. Concentration of H obtained by FTIR and by HI–ERDA, for the films deposited at $R=1.6$ and $R=5.0$, and calculated concentration of N–H bonds, for the films deposited at $R=5.0$, as a function of the composition parameter α_0.

ship between the Si–H bond concentration and the O and N concentrations. The Si–H concentration is shown in Fig. 3 as a function of the N concentration for the films deposited at $R=1.6$. (No Si–H bonds were detected for the films deposited at $R=5.0$). A linear relationship of the type

$$[\mathrm{Si–H}]_{\mathrm{FTIR}}=C_{\mathrm{SiH}}[\mathrm{N}] \tag{7a}$$

is observed, with

$$C_{\mathrm{SiH}}=0.035\pm0.004. \tag{7b}$$

The fit is shown as a dashed line in Fig. 3. As in the case of the N–H bonds, the sample with the highest N concentration deviates from the general trend and was not taken into account for the fitting.

It must be remarked that the relationship given by Eq. (7a) is not an intrinsic property of the $SiO_xN_yH_z$, but a consequence of the particular deposition conditions used in this sample series, as explained earlier.

Figure 4 shows the wave number of the Si–H and N–H stretching bands as a function of the composition parameter α_0. Both bands show a single peak which shifts to higher wave numbers as the composition changes from SiN_yH_z to SiO_2. This behavior is characteristic of single-phase homogeneous $SiO_xN_yH_z$, and is due to the higher electronegativity of O with respect to N.[1,26,27] It is concluded that the H is not incorporated in any specific configuration, but the Si–H and N–H bonds appear with different chemical environments, as determined by the random bonding model and the composition of the films.

C. Comparison of H content obtained by FTIR and HI–ERDA

The total H concentration ([Si–H]+[N–H]) calculated from the Si–H and N–H stretching bands [Eq. (5)] is compared to the total H concentration measured by HI–ERDA in Fig. 5. The line labeled as "N–H (calculated)" will be discussed in a following section. Both measurements are in good agreement. However, it must be noted that the FTIR technique detects only the H present in a bonded state, while the HI–ERDA measurements detects all H in the film, regardless of its bonding state. Keeping this in mind, the agreement observed in Fig. 5 may be understood in two possible ways. First, all H may be in a bonded state so that the FTIR technique would be indeed accounting for all the H in the film. Second, the calibration factor provided by Lanford and Rand may be overestimating the bonded H and be somehow including nonbonded H in addition to the bonded H. This is possible because the calibration factor was determined using nuclear reaction analysis as a reference, which also accounts for all H, without making any distinction between bonded H and nonbonded H.[25] This subject will be thoroughly discussed in the following section.

Another important issue concerning the calibration factor is that it was determined for SiN_yH_z films, although it is also frequently used for $SiO_xN_yH_z$ films.[1,3,8] We have calculated the equivalent calibration factor (Cf_{eq}) using the H concentration measured by HI–ERDA ($[H]_{\mathrm{HI–ERDA}}$) as a reference, in the following way:

$$\mathrm{Cf_{eq}}=\frac{[\mathrm{H}]_{\mathrm{HI–ERDA}}}{(A_{\mathrm{SiH}}+1.4A_{\mathrm{NH}})/d}. \tag{8}$$

A_{SiH}, A_{NH}, and d have the same meaning as in Eq. (5). For this calculation the relative factor 1.4 for the two bands calculated by Lanford and Rand[25] was assumed not to depend on the composition.

The result is shown in Fig. 6 as a function of the composition parameter α_0. The value provided by Lanford and

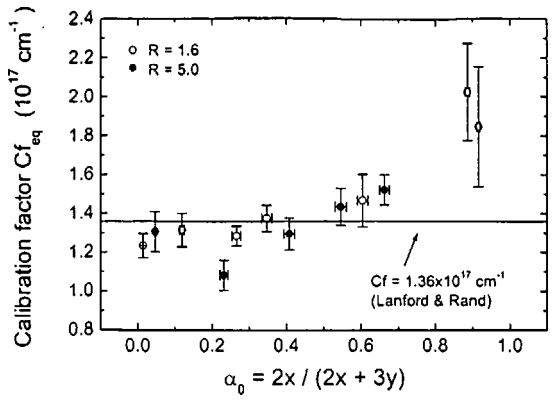

FIG. 6. Equivalent calibration factor, calculated according to Eq. (8), as a function of the composition parameter α_0.

Rand ($C_f = 1.36 \times 10^{17}$ cm^{-1})[25] is plotted as a solid line for comparison. The calculated equivalent calibration factor (Cf_{eq}) remains roughly constant for compositions in the $\alpha_0 = 0-0.5$ range, but a trend for Cf_{eq} to increase is observed for higher values of α_0, especially for the compositions closest to SiO_2. This result suggests a slight dependence of the calibration factor on the composition. The shift of the H related bands to higher wave numbers as the composition changes from SiN_yH_z to SiO_2 (see Fig. 4) supports the conclusion that the properties of these bands depend on the composition.

D. Influence of H on the composition

In this section it will be discussed how the composition is affected by the presence of H, and how it deviates from the stoichiometric behavior [Eqs. (1)–(2)]. The definition of the composition parameter α_0 [Eq. (3)] will also be reviewed.

1. Films deposited at R=5.0

First, we will consider the films deposited at $R=5.0$, in which only N–H bonds were detected. According to the FTIR results, with the N–H band area being proportional to the N concentration (see Fig. 3), a concentration of N–H bonds proportional to the N atom concentration will be assumed.

$$[\text{N–H}] = K_{\text{NH}}[\text{N}]. \tag{9}$$

It must be noted that the proportionality constant K_{NH} in Eq. (9) is not necessarily the same that was calculated in the fit shown in Fig. 3, [C_{NH} in Eqs. (6a) and (6c)]. The C_{NH} value in Eq. (6c) was calculated using the calibration factor given by Lanford and Rand. As discussed earlier, this calibration factor may include not only the N–H bond concentration, but also nonbonded H present in the film. On the other hand, the K_{NH} factor in Eq. (9) accounts for the actual N–H concentration.

In order to take into account the presence of N–H bonds, Eqs. (1a), (1b), and (1c) must be modified as follows:

$$4[\text{Si}] = [\text{Si–O}] + [\text{Si–N}], \tag{10a}$$

$$2[\text{O}] = [\text{Si–O}], \tag{10b}$$

$$3[\text{N}] = [\text{Si–N}] + [\text{N–H}] = [\text{Si–N}] + K_{\text{NH}}[\text{N}], \tag{10c}$$

and the relationship between $x=[\text{O}]/[\text{Si}]$ and $y=[\text{N}]/[\text{Si}]$ derived from Eqs. (10a), (10b), and (10c) is

$$2x + (3 - K_{\text{NH}})y = 4. \tag{11}$$

This result can be understood in terms of a decrease of the effective coordination number of N to form Si–N bonds from 3 to $3-K_{\text{NH}}$, as a consequence of the presence of N–H bonds.[9]

A plot of x as a function of y for the films deposited at $R=5.0$ is shown in Fig. 7 (down). The dashed line corresponds to the stoichiometric relationship [Eq. (2)], and the solid line to the linear fit to Eq. (11). The fit yields the following value for the K_{NH} factor:

$$R = 5.0: \quad K_{\text{NH}} = 0.21 \pm 0.06. \tag{12}$$

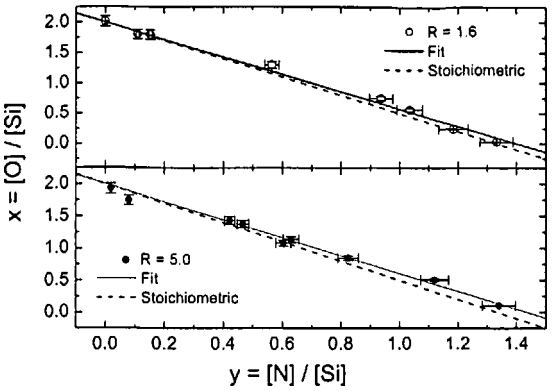

FIG. 7. $x=[\text{O}]/[\text{Si}]$ as a function of $y=[\text{N}]/[\text{Si}]$, obtained by HI–ERDA, for the films deposited at $R=1.6$ (up) and at $R=5.0$ (down). The solid lines are the linear fits to equation 18 ($R=1.6$) and Eq. (11) ($R=5.0$). The dashed lines represent the stoichiometric relationship [Eq. (2)].

This value is lower than the one obtained earlier using the calibration factor of Lanford and Rand [$C_{\text{NH}} = 0.315 \pm 0.011$, Eq. (6c)]. This means that the calibration factor of Lanford and Rand indeed overestimates the actual N–H bond concentration, as we outlined earlier.

The method used in this section allows us to calculate the actual N–H bond concentration, using Eq. (9), the obtained value for K_{NH} [Eq. (12)], and the N concentration measured by HI–ERDA. The result is shown in Fig. 5, as a solid line, together with the H concentrations obtained by HI–ERDA, and by FTIR following the method of Lanford and Rand. This plot evidences the presence of non bonded H in our $SiO_xN_yH_z$ films, especially for compositions close to SiN_yH_z (low values of α_0). Very similar results were previously reported by He *et al.* for $SiO_xN_yH_z$ films deposited by radio frequency PECVD.[9]

Owing to the deviation from the stoichiometric composition as a consequence of the presence of N–H bonds, the composition parameter α_0 [Eq. (3)] should be modified to include this effect. The parameter, understood as the oxide fraction in the $SiO_xN_yH_z$, will be still defined as the fraction of Si–O bonds with respect to the total number of Si bonds. However, due to the decrease of the effective coordination number of N to produce Si–N bonds, [see Eqs. (10c) and (11)], the parameter expressed as a function of x and y is now:

$$\alpha_1 = \frac{[\text{Si–O}]}{[\text{Si–O}] + [\text{Si–N}]} = \frac{2x}{2x + (3 - K_{\text{NH}})y}. \tag{13}$$

The $SiO_xN_yH_z$ formula can be written in terms of α_1 in an analogous way to Eq. (4):

$$SiO_xN_yH_z \leftrightarrow (SiO_2)_{\alpha_1}(SiN_aH_b)_{1-\alpha_1}; \quad a = \frac{4}{3 - K_{\text{NH}}}. \tag{14}$$

The index b should include all H present in the film. Using the H and N concentrations measured by HI–ERDA, and the value obtained for K_{NH} [Eq. (12)], we obtain for the films deposited at $R=5.0$:

$$R=5.0: \quad b=a\times\frac{[\mathrm{H}]}{[\mathrm{N}]}=0.430\pm0.016. \tag{15}$$

(The [H]/[N] ratio was obtained from a linear fit of the HI–ERDA results).

In Eq. (14), the H present in the $SiO_xN_yH_z$ films has been considered to be part of the nitride fraction, because the concentration of H is proportional to the concentration of N; or, in other words, the incorporation of H is correlated to the incorporation of N.

Note also that the index a in Eq. (14), which relates the N and Si concentrations in the nitride fraction, is higher than the equivalent index for H-free stoichiometric SiO_xN_y films [$a=4/3$, as shown in Eq. (4)]. In other words, the relative N content with respect to Si in those films containing N–H bonds is higher than in stoichiometric films. Therefore, we will call these $SiO_xN_yH_z$ films with N–H bonds ''N-rich.'' This term refers to the relative N concentration, as explained earlier. In the next section we will discuss the influence of H on the absolute concentrations of Si, O, and N.

2. Films deposited at $R=1.6$

The discussion for the $SiO_xN_yH_z$ films deposited at $R=1.6$ is analogous to the previous case, but the presence of Si–H bonds must also be taken into account. As explained earlier [see Fig. 3, and Eqs. (7a) and (7b)], the Si–H concentration in our $SiO_xN_yH_z$ films is proportional to the N content rather than proportional to the Si content. Therefore, in addition to the N–H concentration [Eq. (9)], we will assume the following relationship for the Si–H bond concentration:

$$[\mathrm{Si–H}]=K_{\mathrm{SiH}}[\mathrm{N}]. \tag{16a}$$

As in the case of the N–H bonds, the proportionality constant (K_{SiH}) is not the same than the one obtained considering the FTIR results and the calibration factor of Lanford and Rand [C_{SiH} in Eqs. (7a) and (7b)]. K_{SiH} accounts exclusively for the H present in Si–H bonds, while C_{SiH} may overestimate this quantity, including also nonbonded H.

As the presence of Si–H bonds is characteristic of Si-rich films, a concentration of Si–Si bonds will also be considered

$$[\mathrm{Si–Si}]=K_{\mathrm{SiSi}}[\mathrm{N}]. \tag{16b}$$

When N–H, Si–H, and Si–Si bonds are taken into account, the relationship between the atomic concentrations and the concentrations of bonds is

$$4[\mathrm{Si}]=[\mathrm{Si–O}]+[\mathrm{Si–}]+[\mathrm{Si–H}]+2[\mathrm{Si–Si}], \tag{17a}$$

$$2[\mathrm{O}]=[\mathrm{Si–O}], \tag{17b}$$

$$3[\mathrm{N}]=[\mathrm{Si–N}]+[\mathrm{N–H}]. \tag{17c}$$

From Eqs. (17a), (17b), and (17c), together with Eqs. (9), (16a), and (16b), the following relationship between $x=[\mathrm{O}]/[\mathrm{Si}]$ and $y=[\mathrm{N}]/[\mathrm{Si}]$ is obtained:

$$2x+[3-(K_{\mathrm{NH}}-K_{\mathrm{SiH}}-2K_{\mathrm{SiSi}})]y=4, \tag{18}$$

which has the same form than the one obtained for the films deposited at $R=5.0$ [Eq. (11)], but with an equivalent effective decrease of the coordination number of N equal to

$$K_{\mathrm{eq}}=K_{\mathrm{NH}}-K_{\mathrm{SiH}}-2K_{\mathrm{SiSi}}. \tag{19}$$

Therefore, the effect of the Si–H and Si–Si bonds is understood as a decrease of the effective coordination number of Si but only from the point of view of the formation of Si–N bonds, while the coordination number of Si to form Si–O bonds is not affected. So, the effect of N–H bonds is attenuated, as shown in Eqs. (18) and (19).

A plot of x as a function of y for the films deposited at $R=1.6$ is shown in Fig. 7 (up). The solid line corresponds to the linear fit to Eq. (18) and the dashed line to the stoichiometric relationship [Eq. (2)]. The fit yields the following value for K_{eq}:

$$K_{\mathrm{eq}}=K_{\mathrm{NH}}-K_{\mathrm{SiH}}-2K_{\mathrm{SiSi}}=0.14\pm0.06. \tag{20}$$

From this fit it is not possible to determine individually the values of K_{NH}, K_{SiH}, and K_{SiSi} for the films deposited at $R=1.6$. However, it looks plausible to accept that the ratio of the concentration of N–H bonds to the area of the N–H stretching band is the same for the films deposited at $R=5.0$ and $R=1.6$, for a given N content. This is equivalent to the assumption that the ratio of the proportionality constants C_{NH} [Eqs. (6a), (6b), and (6c)] to K_{NH} [Eqs. (9) and (12)] is the same for both series of samples. [Note that the $[\mathrm{N–H}]_{\mathrm{FTIR}}$ quantity in Eq. (6a) is obtained by multiplying the area of the N–H stretching band by the calibration factor of Lanford and Rand, as shown in Eq. (5)]. So

$$\left.\frac{C_{\mathrm{NH}}}{K_{\mathrm{NH}}}\right|_{R=5.0}=\left.\frac{C_{\mathrm{NH}}}{K_{\mathrm{NH}}}\right|_{R=1.6}. \tag{21}$$

Then we can estimate K_{NH} for the films deposited at $R=1.6$:

$$R=1.6: \quad K_{\mathrm{NH}}\approx0.20, \tag{22}$$

which is very close to the value obtained for $R=5.0$ [Eq. (12)], as it is expected when comparing the areas of the N–H bands in both series (see Fig. 3).

We may also accept for the films deposited at $R=1.6$ that the ratio between the area of the Si–H stretching band and the concentration of Si–H bonds is the same than the ratio between the area of the N–H band and the concentration of N–H bonds, except for the relative factor 1.4 calculated by Lanford and Rand.[25] Then

$$\left.\frac{A_{\mathrm{SiH}}}{1.4A_{\mathrm{NH}}}\right|_{R=1.6}=\left.\frac{C_{\mathrm{SiH}}}{C_{\mathrm{NH}}}\right|_{R=1.6}=\left.\frac{K_{\mathrm{SiH}}}{K_{\mathrm{NH}}}\right|_{R=1.6}. \tag{23}$$

Using Eqs. (6b), 7(b), and (22), K_{SiH} is estimated to be

$$R=1.6: \quad K_{\mathrm{SiH}}\approx0.02. \tag{24}$$

And from Eq. (20):

$$R=1.6: \quad K_{\mathrm{SiSi}}\approx0.02. \tag{25}$$

Although this calculation is just estimation, it shows that the FTIR results are quantitatively consistent with the model proposed along this section. Additionally, it has been possible to estimate the concentration of Si–Si bonds to be of the same order than the concentration of Si–H bonds.

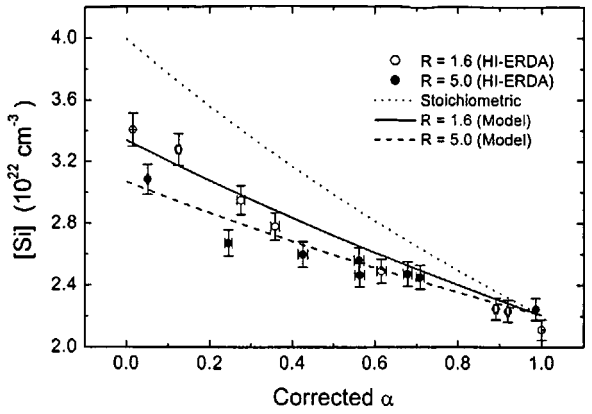

FIG. 8. Absolute atomic concentration of Si, measured by HI–ERDA, for the films deposited at $R=1.6$ and $R=5.0$, as a function of the corrected composition parameter α [α_1 in Eq. (13) for $R=5.0$ or α_2 in Eq. (26) for $R=1.6$]. The concentration for stoichiometric $SiO_xN_yH_z$ is shown as a dotted line, and the concentrations predicted by our model are shown as solid ($R=1.6$) and dashed ($R=5.0$) lines.

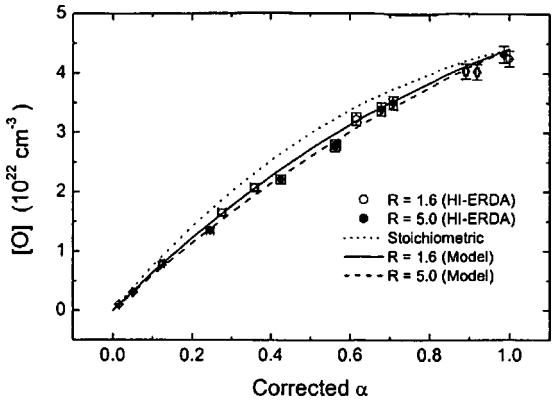

FIG. 9. Absolute atomic concentration of O, measured by HI–ERDA, for the films deposited at $R=1.6$ and $R=5.0$, as a function of the corrected composition parameter α [α_1 in Eq. (13) for $R=5.0$ or α_2 in Eq. (26) for $R=1.6$]. The concentration for stoichiometric $SiO_xN_yH_z$ is shown as a dotted line, and the concentrations predicted by our model are shown as solid ($R=1.6$) and dashed ($R=5.0$) lines.

Finally, for the films deposited at $R=1.6$, the composition parameter α can be also modified in an analogous way as in the case of $R=5.0$ [Eq. (13)], but replacing K_{NH} by K_{eq} [Eq. (20)]:

$$\alpha_2=\frac{[\text{Si–O}]}{[\text{Si–O}]+[\text{Si–N}]+[\text{Si–H}]+2[\text{Si–Si}]}$$

$$=\frac{2x}{2x+(3-K_{eq})y}. \tag{26}$$

The meaning of α_2 is still the fraction of Si–O bonds with respect to the total Si bonds, but now the Si–H and Si–Si bonds are also considered.

The $SiO_xN_yH_z$ formula can be written in terms of α_2:

$$SiO_xN_yH_z \leftrightarrow (SiO_2)_{\alpha_2}(SiN_aH_b)_{1-\alpha_2}; \quad a=\frac{4}{3-K_{eq}}. \tag{27}$$

For the films deposited at $R=1.6$ the index b was calculated to be

$$R=1.6: \quad b=0.466\pm0.015. \tag{28}$$

E. Influence of H on the absolute atomic concentrations of Si, O, and N

In the previous section it has been shown how the presence of N–H, Si–H, and Si–Si bonds results in deviations with respect to the stoichiometric composition in terms of the relative concentrations of Si, O, and N. In this section, we will study the influence of H on the absolute atomic concentrations.

Figures 8, 9, and 10 show the absolute atomic concentrations of Si, O, and N, respectively, measured by HI–ERDA, for the films deposited at $R=1.6$ and $R=5.0$, as a function of the composition parameter α. In these plots the corrected values α_1 [Eq. (13)] or α_2 [Eq. (26)] were used for the films deposited at $R=5.0$ and $R=1.6$, respectively. The expected Si, O, and N concentrations for stoichiometric SiO_xN_y are also shown as dotted lines for comparison. These concentrations were calculated using $\rho=2.2$ g/cm^3 for SiO_2,[28] and $\rho=3.1$ g/cm^3 for Si_3N_4,[28] and assuming a linear dependency of the density on the composition parameter α_0.

As shown in the figures, the measured Si, O, and N compositions are lower than those calculated for stoichiometric films. In the case of Si and N, the difference is more significant for compositions close to SiN_yH_z ($\alpha=0$), while in the case of O, the larger difference is observed for intermediate compositions. This behavior is explained by the presence of H, which is incorporated at the expense of Si, O, or N atoms. Figure 11 shows the difference between the stoichiometric Si atomic concentration and the measured Si concentration $\Delta[\text{Si}]=[\text{Si}]_0-[\text{Si}]_{\text{HI–ERDA}}$, for the films deposited at $R=1.6$ and $R=5.0$, as a function of the concentration of N. (The corresponding stoichiometric Si concentration for a given sample is calculated assuming an α_0 value for the stoichiometric film equal to corrected composition parameter α of the sample.)

A linear relation is observed between Δ[Si] and [N]:

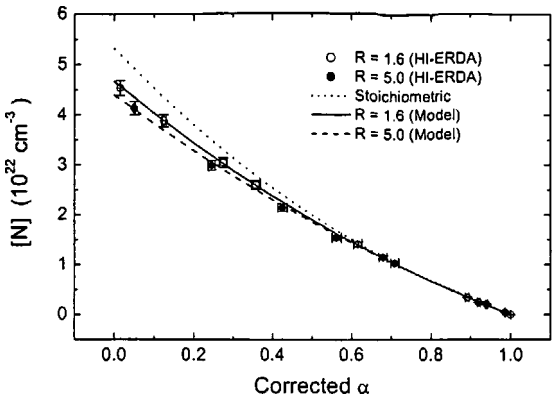

FIG. 10. Absolute atomic concentration of N, measured by HI–ERDA, for the films deposited at $R=1.6$ and $R=5.0$, as a function of the corrected composition parameter α [α_1 in Eq. (13) for $R=5.0$ or α_2 in Eq. (26) for $R=1.6$]. The concentration for stoichiometric $SiO_xN_yH_z$ is shown as a dotted line, and the concentrations predicted by our model are shown as solid ($R=1.6$) and dashed ($R=5.0$) lines.

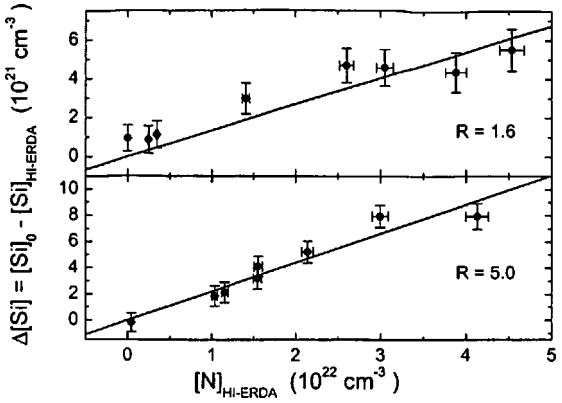

FIG. 11. Difference between the expected Si atomic concentration for stoichiometric SiO_xN_y films ($[Si]_0$) and the Si concentration measured in our $SiO_xN_yH_z$ films by HI–ERDA ($[Si]_{HI-ERDA}$), as a function of the measured N concentration. Solid lines correspond to the linear fit of the data to Eq. (29).

$$\Delta[Si]=B[N]. \tag{29}$$

The lines in Fig. 11 correspond to the linear fits of the data with Eq. (29). The following values were obtained for the proportionality constant B for each sample series:

$$R=5.0: \quad B=0.221\pm0.013, \tag{30a}$$

$$R=1.6: \quad B=0.135\pm0.012. \tag{30b}$$

The values obtained here for the films deposited at $R=5.0$ and $R=1.6$ are the same as the ones obtained above for K_{NH} [Eq. (12), $K_{NH}=0.21\pm0.06$] and K_{eq} [Eq. (20), $K_{eq}=0.14\pm0.06$], respectively.

In the case of the films deposited at $R=5.0$, this result means that the difference in the Si atom concentration with respect to the stoichiometric film equals the N–H concentration [see Eqs. (9) and (29)]. Therefore, it is concluded that the incorporation of H in the form of N–H bonds takes place at the expense of Si atoms. In other words, each H atom forming a N–H bond replaces a Si atom, with respect to the stoichiometric film, thus reducing the absolute Si atom concentration, as shown in Fig. 8. The decrease of the Si atom concentration, in turn, results in lower concentrations of O and N with respect to the stoichiometric films (Figs. 9 and 10). For the films deposited at $R=1.6$ the interpretation of the result is not so straightforward because K_{eq} also includes the effect of Si–H and Si–Si bonds [see Eq. (19)].

In the following, a model based on these results is developed to explain quantitatively the differences between the measured Si, O, and N concentrations and those expected for stoichiometric SiO_xN_y films with the same composition parameter α.

1. Films deposited at R=5.0

As explained earlier, the influence of N–H bonds on the $SiO_xN_yH_z$ films deposited at $R=5.0$ is a replacement of Si atoms by H atoms, with respect to the stoichiometric film. Therefore, according to our model, the Si atom concentration ([Si]) in the films deposited at $R=5.0$ may be calculated from the stoichiometric Si concentration ($[Si]_0$) in the following way:

$$[Si]=[Si]_0-[N\text{–}H]=[Si]_0-K_{NH}[N], \tag{31a}$$

where Eq. (9) was taken into account. Equation (31a) implies a decrease of the Si atom concentration with respect to the stoichiometric concentration. As O and N are incorporated in the form of Si–O and Si–N bonds, the O and N atom concentrations should be decreased accordingly. In the case of O, the decrease of the atomic concentration equals the number of Si–O bonds lost as a consequence of the Si concentration decrease, divided by 2, which is the coordination number of O. Taking into account the meaning of the composition parameter α_0 [Eq. (3)], the number of Si–O bonds lost is $4\Delta[Si]=4\alpha_0K_{NH}[N]$ and the O concentration in our model is

$$[O]=[O]_0-\frac{4\alpha_0K_{NH}[N]}{2}. \tag{31b}$$

A decrease of the N atom concentration is also expected, with the number of Si–N bonds lost being $4(1-\alpha_0)K_{NH}[N]$. However, N–H bonds are gained with respect to the stoichiometric film. Therefore, our model yields for the N atom concentration

$$[N]=[N]_0-\frac{4(1-\alpha_0)K_{NH}[N]}{3}+\frac{K_{NH}[N]}{3}. \tag{31c}$$

Note that the parameter α_0 appearing in Eqs. (31b) and (31c) corresponds to the definition for stoichiometric films [Eq. (3)]. However, it is possible to calculate the corresponding corrected parameter α_1 [Eq. (13)] using the expressions of [O] and [N] given by Eqs. (31b) and (31c), and taking into account the relationship between $[O]_0$, $[N]_0$, and α_0 [see Eq. (4)]:

$$\frac{[O]_0}{[N]_0}=\frac{2\alpha_0}{4(1-\alpha_0)/3}. \tag{32}$$

The α_1 value obtained in this way equals α_0. So, our model allows to calculate the Si, O, and N atom concentrations for a $SiO_xN_yH_z$ film characterized by a composition parameter α_1, taking a stoichiometric SiO_xN_y film with $\alpha_0=\alpha_1$ as a reference. First, [N] is computed from Eq. (31c) and then [Si] and [O] are obtained from Eqs. (31a) and (31b), respectively. The proportionally constant K_{NH} was also previously calculated [Eq. (12)].

The calculated concentrations following this model are shown in Figs. 8, 9, and 10, together with the measured values. A perfect agreement between the model and the experiment is observed.

Note that according to Eq. (14), the concentrations of O and N may also be calculated as

$$[O]=2\alpha_1[Si], \tag{33a}$$

$$[N]=\frac{4}{3-K_{NH}}(1-\alpha_1)[Si]. \tag{33b}$$

Keeping in mind that α_1 equals α_0, as explained earlier, the definition of α_0 [Eq. (3)], and the relationship between the stoichiometric compositions $[Si]_0$, $[O]_0$, and $[N]_0$ [Eq. (2)], it can be shown that Eqs. (33a) and (33b) are equivalent to Eqs. (31b) and (31c), respectively.

Finally, concerning the presence of nonbonded H, the substitution of Si atoms by H atoms forming N–H bonds, with the subsequent decrease of the O and N atom concentrations, results in a lower film density with respect to the stoichiometric SiO_xN_y, possibly appearing microvoids where H may be present in a nonbonded state. So, it is suggested that the presence of nonbonded H is related to the presence of N–H bonds, and the associated decrease of the film density.

2. Films deposited at R=1.6

For the films deposited at $R=1.6$ the SiH_4 partial pressure during deposition is higher than in the case of $R=5.0$ and the Si content for a given value of the composition parameter is higher, as shown in Fig. 8. This is also evidenced by the presence of Si–H bonds, although the N–H concentration is much higher than the Si–H concentration, so that these films may be also regarded as N-rich (the index a relating the N and Si concentrations in Eq. (27) is higher than the stoichiometric 4/3). The incorporation of H in the form of N–H bonds has the same effect as in the case of $R=5.0$. However, according to the fitting result obtained earlier [Fig. 11 and Eqs. (29) and (30b)], for the films deposited at $R=1.6$, the number of Si atoms replaced by H atoms with respect to the stoichiometric film is not equal to the concentration of N–H bonds ($[N–H]=K_{NH}[N]$) but to the concentration of N–H bonds minus the number of Si bonds involved in Si–H and Si–Si bonds

$$\Delta[Si]=[Si]_0-[Si]=[N–H]-[Si–H]-2[Si–Si]$$
$$=K_{eq}[N]. \quad (34)$$

This result may be understood in the following way. Each N–H bond substitutes a Si–N bond in the stoichiometric film. For the films deposited at $R=5.0$, with no Si–H or Si–Si bonds, this results in the H atom actually replacing the Si atom. However, in the films deposited at $R=1.6$, each Si–H bond provides an additional Si bond, so that the broken Si–N bond may result in a new N–H bond and a new Si–H bond with respect to the stoichiometric film, with no replacement of Si by H. Similarly, two broken Si–N bonds may result in two N–H bonds and one Si–Si bond with no decrease of the Si concentration. The exact mechanism leading to this network configuration with a higher Si content than in the films deposited at $R=5.0$ is unknown. However, it seems quite clear that it is a consequence of the higher SiH_4 partial pressure during the deposition with $R=1.6$.

It must also be noted that the effect of the Si–H and Si–Si bonds described here must be considered within a network in which a high concentration of N–H bonds is present, leading to a decrease of the density of the film with respect to the stoichiometric one. The effect of Si–H bonds in a film without N–H bonds may be different than the one observed in this work. This subject will be investigated in the future.

The concentration of Si, O, and N for the films deposited at $R=1.6$ may be calculated following the same model used for $R=5.0$, but replacing. K_{NH} by K_{eq}, so that the effect of Si–H and Si–Si bonds is included. [Note that in Eq. (31c) replacing K_{NH} by K_{eq} means subtracting those Si bonds which are not forming Si–N bonds, but Si–H or Si–Si bonds.]

The result is shown in Figs. 8, 9, and 10, for the Si, O, and N atom concentrations, respectively, again with a perfect agreement between the model and the experimental data.

IV. CONCLUSIONS

The incorporation of H in ECR-deposited $SiO_xN_yH_z$ films was studied in detail. The H content (both N–H and Si–H bonds) was found to be proportional to the N content of the films, for each series of samples deposited at a given value of the parameter $R=[\phi(O_2)+\phi(N_2)]/\phi(SiH_4)$. The deviation from the stoichiometric H-free SiO_xN_y composition due to the presence of N–H bonds was studied. The presence of N–H bonds results in a decrease of the effective coordination number of N to produce Si–N bonds, thus resulting in a higher N to Si ratio than in stoichiometric films. By fitting the experimental data, it was possible to determine the actual content of bonded H. With this calculation, the presence of H in a nonbonded state was made evident. Additionally, by comparing the H content obtained from the Si–H and N–H stretching absorption bands measured by FTIR spectroscopy with the results obtained by HI–ERDA, it was shown that calibration factors should be handled with care, as they may include not only the bonded H, but also nonbonded H. The presence of Si–H and Si–Si bonds was also studied and found to partially compensate the effect of the N–H bonds.

The absolute atom concentrations of Si, O, and N, measured by HI–ERDA, were compared with the calculated ones for stoichiometric SiO_xN_y films. It was shown that N–H bonds are formed at the expense of Si–N bonds, with each H atom replacing a Si atom, resulting in a lower atomic concentration than in the stoichiometric film. The presence of Si–H and Si–Si bonds was linked to a lower decrease of the Si concentration with respect to the stoichiometric film.

Finally, a model was developed to calculate the expected Si, O, and N concentrations taking into account the influence of N–H, Si–H, and Si–Si bonds. The predictions of the model were in perfect agreement with the experimental data.

ACKNOWLEDGMENTS

The authors acknowledge C. A. I. de Implantación Iónica (U. C. M.) for availability of the deposition system. C. A. I. of Espectroscopia (U. C. M.) is acknowledged for availability of FTIR spectrometer. The work has been partially financed by the CICYT (Spain) under Contract No. TIC 01-1253. Technical support of G. Keiler (HMI) is gratefully acknowledged.

[1] Y. Ma and G. Lucovsky, J. Vac. Sci. Technol. B **12**, 2504 (1994).
[2] T. Arakawa, R. Matsumoto, and A. Kita, Jpn. J. Appl. Phys., Part 1 **35**, 1491 (1996).
[3] W. A. P. Claassen, H. A. J. Th. v. d. Pol, A. H. Goemans, and A. E. T. Kuiper, J. Electrochem. Soc. **133**, 1458 (1986).
[4] J.-H. Kim *et al.*, J. Vac. Sci. Technol. A **18**, 1401 (2000).
[5] P. V. Bulkin, P. L. Swart, and B. M. Lacquet, J. Non-Cryst. Solids **187**, 484 (1995).

[6] S. Callard, A. Gagnaire, and J. Joseph, J. Vac. Sci. Technol. A **15**, 2088 (1997).
[7] F. Galliard, P. Schiavone, and P. Brault, J. Vac. Sci. Technol. A **15**, 2777 (1997).
[8] C. M. M. Denisse, K. Z. Troost, J. B. Oude Elferink, F. H. P. M. Habraken, W. F. van der Weg, and M. Hendriks, J. Appl. Phys. **60**, 2536 (1986).
[9] L.-N. He, T. Inokuma, and S. Hasegawa, Jpn. J. Appl. Phys., Part 1 **35**, 1503 (1996).
[10] S. V. Hattangady, H. Niimi, and G. Lucovsky, J. Vac. Sci. Technol. A **14**, 3017 (1996).
[11] M. Hernández Vélez, O. Sánchez Garrido, F. Fernández Gutiérrez, C. Falcony, and J. M. Martínez-Duart, J. Vac. Sci. Technol. B **16**, 1087 (1998).
[12] D. Landheer, Y. Tao, J. E. Hulse, T. Quance, and D.-X. Xu, J. Electrochem. Soc. **143**, 1681 (1996).
[13] M. J. Hernández, J. Garrido, J. Martínez, and J. Piqueras, Semicond. Sci. Technol. **12**, 927 (1997).
[14] A. del Prado, I. Mártil, M. Fernández, and G. González-Díaz, Thin Solid Films **343–344**, 432 (1999).
[15] A. Sassella, P. Lucarno, A. Borghesi, F. Corni, S. Rojas, and L. Zanotti, J. Non-Cryst. Solids **187**, 395 (1995).
[16] C. M. M. Denisse, K. Z. Troost, F. H. P. M. Habraken, W. F. van der Weg, and M. Hendriks, J. Appl. Phys. **60**, 2543 (1986).
[17] A. del Prado, E. San Andrés, I. Mártil, G. González-Díaz, D. Bravo, F. J. López, M. Fernández, and F. L. Martínez, J. Appl. Phys. **94**, 1019 (2003).
[18] S. García, J. M. Martín, M. Fernández, I. Mártil, and G. González-Díaz, Philos. Mag. B **73**, 487 (1996).
[19] F. L. Martínez *et al.*, Phys. Rev. B **63**, 245320 (2001).
[20] F. L. Martínez, I. Mártil, G. Gomzález-Díaz, B. Selle, and I. Sieber, J. Non-Cryst. Solids **227–230**, 523 (1998).
[21] A. del Prado *et al.*, J. Appl. Phys. **93**, 8930 (2003).
[22] W. Bohne, J. Röhrich, and G. Röschert, Nucl. Instrum. Methods Phys. Res. B **136–138**, 633 (1998).
[23] W. Bohne *et al.*, Surf. Interface Anal. **34**, 749 (2002).
[24] A. Sassella, Phys. Rev. B **48**, 14208 (1993).
[25] W. A. Lanford and M. J. Rand, J. Appl. Phys. **49**, 2473 (1978).
[26] G. Lucovsky, Solid State Commun. **29**, 571 (1979).
[27] D. V. Tsu, G. Lucovsky, and B. N. Davidson, Phys. Rev. B **40**, 1795 (1989).
[28] S. M. Sze, *Physics of Semiconductor Devices* (Wiley, New York, 1981).